Journal of Materials Chemistry B

Orthogonal click reactions enable the synthesis of ECM-mimetic PEG hydrogels without multi-arm precursors

Journal:	*Journal of Materials Chemistry B*
Manuscript ID	TB-ART-05-2018-001399.R1
Article Type:	Paper
Date Submitted by the Author:	05-Jul-2018
Complete List of Authors:	Jivan, Faraz; Texas A&M University, Biomedical Engineering Fabela, Natalia; Texas A&M University, Biomedical Engineering Davis, Zachary; North Carolina State Univeristy, Materials Science and Engineering Alge, Daniel; Texas A&M University, Biomedical Engineering; Texas A&M University, Materials Science and Engineering

Journal of Materials Chemistry B

Paper

Orthogonal click reactions enable the synthesis of ECM-mimetic PEG hydrogels without multi-arm precursors

Received 14th May 2018,
Accepted 00th June 2018

DOI: 10.1039/x0xx00000x

www.rsc.org/

Faraz Jivan[a], Natalia Fabela[a], Zachary Davis[b] and Daniel L. Alge[a,c]

Click chemistry reactions have become an important tool for synthesizing user-defined hydrogels consisting of poly(ethylene glycol) (PEG) and bioactive peptides for tissue engineering. However, because click crosslinking proceeds via a step-growth mechanism, multi-arm telechelic precursors are required, which has some disadvantages. Here, we report for the first time that this requirement can be circumvented to create PEG-peptide hydrogels solely from linear precursors through the use of two orthogonal click reactions, the thiol-maleimide Michael addition and thiol-norbornene click reaction. The rapid kinetics of both click reactions allowed for quick formation of norbornene-functionalized PEG-peptide block copolymers via Michael addition, which were subsequently photocrosslinked into hydrogels with a dithiol linker. Characterization and *in vitro* testing demonstrated that the hydrogels have highly tunable physicochemical properties and excellent cytocompatiiblity. In addition, stoichiometric control over the crosslinking reaction can be leveraged to leave unreacted norbornene groups in the hydrogel for subsequent hydrogel functionalization via bioorthogonal inverse-electron demand Diels-Alder click reactions with *s*-tetrazines. After selectively capping norbornene groups in a user-defined region with cysteine, this feature was leveraged for protein patterning. Collectively, these results demonstrate that our novel chemical strategy is a simple and versatile approach to the development of hydrogels for tissue engineering that could be useful for a variety of applications.

1. Introduction

Hydrogels are crosslinked hydrophilic polymer networks that are considered to be the most tissue-like class of biomaterials, which has led to high interest in their use for tissue engineering.[1-3] Common crosslinking strategies to fabricate hydrogels include physical crosslinking through polymer chain entanglements or electrostatic interactions, and chemical crosslinking between functional groups. Within chemical crosslinking, chain growth polymerization through rapid propagation of a radical center is widely used with acrylate-containing polymers. However, this approach lacks control and reaction specificity due to the potential for chain transfer events, which can damage proteins and cells.[4-6] Alternatively, step growth polymerization between two distinct complementary chemical groups allows for more predictable crosslinking and is amenable to a wide range of chemical handles.[7, 8] Click chemistry is widely appreciated as a tool for controlling the step-growth crosslinking of hydrogels. The efficiency, functional group selectivity, and mild nature of click-type reactions makes them particularly well suited for hydrogels being synthesized in the presence of fragile cells or biologics.[9-12]

There has been considerable innovation in the synthesis of extracellular matrix (ECM)-mimetic hydrogels by click chemistry from both naturally-occurring and synthetic polymers. Hyaluronic acid and gelatin, both natural polymers which already contain cellular binding domains, have been chemically modified along their respective polymer backbones to incorporate click functional groups for pendant peptide or ECM protein functionalization and to provide numerous crosslinking sites that can be used to independently tune hydrogel mechanical properties.[13-18] Synthetic hydrogels based on poly(ethylene glycol) (PEG) have widely been used in tissue engineering because of their hydrophilicity, tunable tissue-like elasticity, and bio-inertness. PEG hydrogels are also considered to be a "blank slate" platform that can be easily modified with peptides and proteins for drug delivery and cell encapsulation.[19] Notably, the use of photo-initiated thiol-ene click reactions,[4, 20, 21] and Michael addition reactions such as the thiol-vinyl sulfone[22, 23] and thiol-maleimide reactions,[24-27] have become increasingly important in the synthesis of complex, user-controlled hydrogel matrices. Additionally, advances have been made in using biorthogonal, initiator-free click reactions such as oxime ligation,[28, 29] strain promoted azide-alkyne click,[30, 31] and tetrazine-norbornene click reactions[32, 33] for facile incorporation of bioactive ECM-

[a] Texas A&M University, Department of Biomedical Engineering, 5045 Emerging Technologies Building, 3120 TAMU, College Station, TX, 77843, United States. *E-mail: dalge@tamu.edu. Fax: 1-979-845-4450. Tel: 1-979-458-9248.
[b] North Carolina State University, Department of Materials Science and Engineering, 911 Partners Way, Raleigh, NC 27606, United States.
[c] Texas A&M University, Department of Materials Science and Engineering, 3003 TAMU, College Station, TX, 77843, United States.

Electronic Supplementary Information (ESI) available: [details of any supplementary information available should be included here]. See DOI: 10.1039/x0xx00000x

mimetic peptides for cell attachment, cellular degradation or directed differentiation.

Due to the step-growth nature of click cross-linking reactions, the synthesis of ECM mimetic PEG-peptide hydrogels with these chemical strategies requires the use of multi-arm, telechelic PEG precursors. These macromers are synthesized by living ring-opening polymerization of ethylene oxide using multi-functional alcohol cores like pentaerythritol.[34] While they are widely used in hydrogel fabrication, there are important drawbacks. For example, steric hindrance of the growing polymer chain and impurities such as water can lead to lower extents of polymerization, unpredictable molecular weights and fewer arms than desired. Achieving quantitative functionalization of the end groups with clickable functional handles is also challenging compared to linear PEG precursors and often requires a large excess of functional reagent, which can be costly. Even post-synthesis, the analytical method for determining functionalization, nuclear magnetic resonance spectroscopy (NMR), can provide an incomplete picture of the chemical structure, because of the large discrepancy between the ratio of end group hydrogens compared to hydrogens in the polymer backbone.[35] These drawbacks are important because they can adversely affect hydrogel properties. Reaction stoichiometry is critical in step-growth reactions and click crosslinking, and variability in the functionality of precursors can reduce the number of sites for conjugation, alter crosslinking density, and result in heterogeneous networks or non-idealities within the polymer structure.[36, 37] Additionally, the fact that PEG can only be functionalized on the chain ends means that conjugation of bioactive molecules takes away potential crosslinking sites, thereby limiting the amount that can be added.

To circumvent these challenges, the objective of this work was to develop an alternative strategy for synthesizing ECM-mimetic hydrogels that utilizes only linear precursors. Specifically, we sought to synthesize PEG-peptide block co-polymers (BCPs) via step-growth polymerization of PEG-di-maleimide with di-cysteine peptides. To render these BCPs crosslinkable, we installed norbornene groups on one of the peptides. Since norbornene is an electron-rich alkene, it will not participate in Michael addition reactions but can readily participate in radical initiated thiol-ene reactions as well as inverse electron demand Diels-Alder reactions with *s*-tetrazines. Here, we demonstrate the ability to tune BCP hydrogel mechanical properties and utilize this versatile platform for cell encapsulation and bioactive protein patterning.

2. Experimental

Materials

PEG di-maleimide (5,000 g/mol) and PEG di-thiol (3,400 g/mol) were purchased from Laysan Bio Inc. Rink amide MBHA resin (100-200 mesh) was purchased from Novabiochem. Fmoc protected amino acids, 2-(1H-benzotriazol-1-yl)-1,1,3,3-tetramethyluronium hexauorophosphate (HBTU), and N-methyl-pyroliddinone (NMP) were purchased from Chem-Impex International Inc. Triethanolamine (TEOA), diisopropyl ethylamine (DIEA), deuterium oxide (D_2O), 5,5'-dithio-bis-(2-nitrobenzoic acid) (DTNB or Ellman's reagent), phenol, piperidine, triisopropylsilane (TIS), trifluoroacetic acid (TFA) reagent grade and HPLC grade were purchased from Sigma Aldrich. L-cysteine, 5-norbornene 2-carboxcylic acid was purchased from Alfa Aesar. Dichloromethane (DCM), HPLC grade water and acetonitrile (ACN) were purchased from Thermo Fisher Scientific. Dulbecco's Modified Eagle Medium (DMEM) was purchased from Corning. Fetal bovine serum (FBS) was purchased from Atlanta Biologicals. Penicillin streptomyosin (Pen Strep) was purchased from Lonza. Calcein-AM and ethidium homodimer-1 were purchased from Life Technologies.

Synthetic Procedures

Synthesis of Peptide Sequences.

General. Peptide synthesis was performed on Rink amide resin with a microwave assisted peptide synthesizer (CEM DiscoverBio) using standard Fmoc solid phase peptide synthesis and HBTU activation with DIEA (0.5 M) in NMP.[38] Coupling reactions were generally performed for 6 min at 75 °C, except for cysteine (C) and arginine (R) which were coupled for 6 min at 50 °C, and 25 min at room temperature then 5 min at 75 °C, respectively. Fmoc protecting groups were deprotected with piperidine (20%) in NMP for 5 min at 75 °C. The peptide was cleaved by treatment with 90:5:2.5:2.5 (TFA:phenol:TIS:water) for 2 hrs at room temperature followed by precipitation in cold diethyl ether. Crude peptide was purified by reverse-phase high performance liquid chromatography (HPLC, Thermo Scientific UltiMate 3000 with Agilent Technologies C18 column, ACN in water with 0.01% TFA) and lyophilized (Supporting Information, Figure S1). Purified product was analyzed via matrix assisted laser desorption ionization time-of-flight mass spectrometry (MALDI-TOF MS) to verify peptide composition (Supporting Information, Figure S2). Peptides were dissolved in PBS and absorbance measurements at 205 nm and 280 nm (Thermo Scientific Nanodrop One) were taken to calculate the stock concentrations.[39] MALDI-TOF MS: KCGPQGIAGQCK [M+H] = 1188.513 (expected), 1189 (found); CGRGDSGC [M+H] = 753.242 (expected), 752.9 (found).

CGK(NB)GC. Norbornene-containing peptide was synthesized as described above, but with slight variation. A lysine residue with a 4-methyltrityl (Mtt) side protecting group (Fmoc-L-lysine(Mtt)-OH) was used during synthesis instead of the traditional lysine residue (Fmoc-L-lysine). After coupling the K(Mtt) residue, the Mtt protecting group was removed by addition of 1.8% TFA in DCM (9 washes, 3 min each at room temperature). The resin was then washed with DCM followed by NMP. Subsequently, 5-norbornene 2-carboxcylic acid was coupled to the free amine group by HBTU coupling (4:4:1 norbornene acid:HBTU:resin) and DIEA (0.5 M) in NMP. The Fmoc protecting group on the lysine residue was then

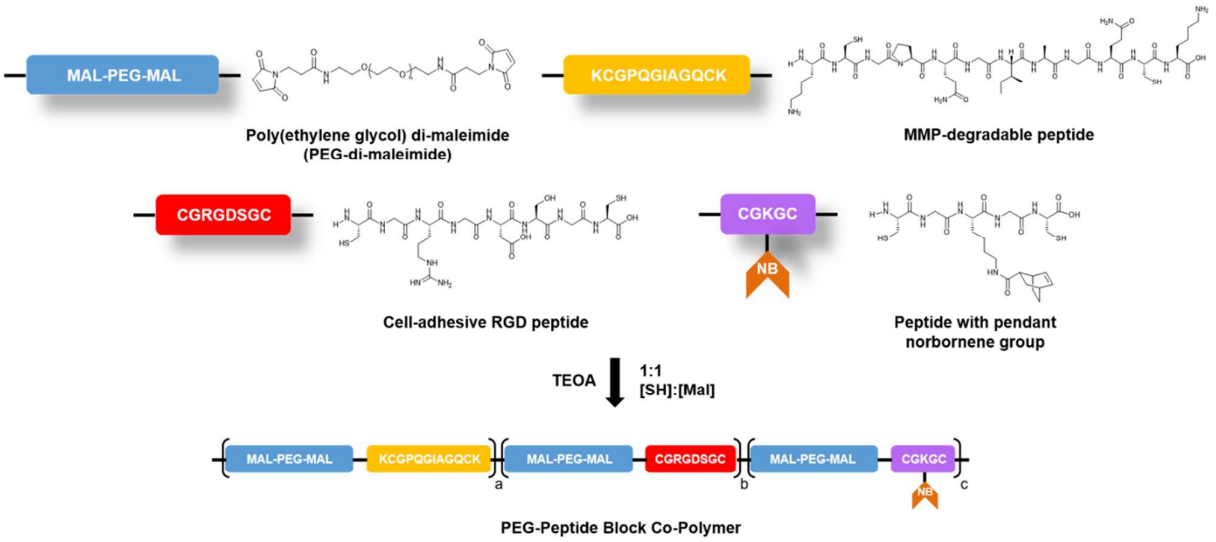

Fig. 1 PEG-Peptide Block Co-Polymer Assembly via Michael Addition. Cartoon representation depicting the assembly process of PEG and peptide subunits into random block-co polymer chains via thiol-maleimide Michael addition of PEG-di-maleimide and di-cysteine containing peptides initiated by triethanolamine. The concentration of each component used to synthesize the block co-polymer chains is shown in Table 1. The subscripts "a – c" correspond to the number of repeat units within the block co-polymer (c = 15b = 3a).

removed using standard deprotection, and peptide synthesis was completed normally, as described above. MALDI-TOF MS: [M+H] = 586 (expected), 586.396 (found).

Synthesis of PEG-Peptide Block Co-Polymer (BCP) Chains.

To prepare the PEG-peptide BCP precursor solution, PEG-di-maleimide was polymerized with di-thiol containing peptide sequences of interest via a Michael addition reaction (Table 1). A large batch (5 mL) of BCP precursor was prepared from lyophilized PEG and peptides. Briefly, linear bifunctional PEG-maleimide (PEG-Mal, 10.5 wt. %), MMP-degradable di-thiol containing peptide KCGPQGIAGQCK (5 mM), cell-adhesive peptide CGRGDSGC (1 mM), and short peptide with a pendant norbornene group CGK(NB)GC (15 mM), were mixed with TEOA in PBS (1 mM, pH 7-9). The polymer mixture was allowed to polymerize for 30 minutes at room temperature to form PEG-peptide BCP (Figure 1).

Synthesis of BCP Hydrogels.

PEG-peptide BCP precursor solutions were subsequently crosslinked via thiol-ene click chemistry. Briefly, block co-polymers were combined with a PEG-di-thiol crosslinker ([thiol]:[norbornene] ratio of 1:1) and lithium acylphosphinate photoinitiator (LAP, 2 mM), synthesized as previously described.[40] Varying dilutions of this BCP pre-polymer solution were prepared in PBS to result in different crosslinking (XL) densities (1:1 = high XL, 1:2 = medium XL, and 1:3 = low XL) (Table 2). Pre-polymer solutions (50 µL) were added to 6 mm syringe-tip molds and photopolymerization was achieved using UV light (Omnicure S2000 with a 365 nm filter) at 10 mW/cm^2 for 5 minutes.

Table 1 Concentration of Components for BCP Chain Formation

Components	Working Concentration of Components	Working Concentration of Click Groups
PEG-Mal	21 mM	42 mM MAL
KCGPQGIAGQCK	5 mM	10 mM SH
CGRGDSGC	1 mM	2 mM SH
CGK(NB)GC	15 mM	30 mM SH and 15 mM NB

Methods

Chemical analysis of PEG-Peptide BCP.

Thiol conversion during BCP polymerization was monitored via Ellman's Assay to determine the extent of the Michael addition polymerization. BCP samples and negative control samples containing PEG-NB instead of PEG-Mal were prepared (n = 3). Samples (10 µL) were taken at various time points (15, 30, 45, and 60 min) and incubated with Ellman's reagent (0.125 mg/mL in PBS, 100 µL). Absorbance measurements at 405 nm were taken, compared to a standard curve of L-cysteine (0 - 2 mM), and thiol concentrations were normalized to negative control sample at 0 minutes. Various sample dilutions were tested to ensure that all measurements taken were within the assay range.

^{1}H NMR Characterization.

^{1}H NMR characterization of the BCP precursor and gels was performed to compare spectra after Michael addition and thiol-ene photopolymerization, respectively. Briefly, BCP Michael addition was performed as previously described and separately a non-gelling photopolymerization BCP reaction with LAP (2 mM) and L-cysteine (15 mM) was performed to consume norbornenes. Samples were frozen at -80 °C and

Table 2 Concentration of Components for BCP Gels

Components	Working Concentration of Click Groups		
	High XL	*Med XL*	*Low XL*
BCP	12 mM NB	6 mM NB	4 mM NB
PEG-di-thiol	12 mM SH	6 mM SH	4 mM SH

lyophilized for 2 days. Lyophilized products (10 mg) were dissolved in D_2O, tested using an Inova NMR Spectrometer (500 MHz, 64 scans) and analysed via MestReNova NMR software (Mestralab Research S.L.).

Swelling Ratios of BCP Gels.

Hydrogel samples were immersed in 2 mL of PBS for 48 hours to reach equilibrium. Swelling ratios of BCP gels were obtained by measuring the mass of dehydrated gels (W_d) and gels swollen in PBS for 2 days (W_s). The formula for calculating swelling ratio is shown below:

$$\boldsymbol{Swelling\ Ratio} = (\boldsymbol{W_s} - \boldsymbol{W_d})/(\boldsymbol{W_d})$$

Rheology of BCP Gels.

To characterize mechanical properties of BCP gels, amplitude time sweep rheology was performed to measure gelation point and storage modulus. To monitor hydrogel gelation, hydrogels were monitored during crosslinking via *in situ* photopolymerization rheology. Briefly, pre-polymer solution (50 µL) was added on a peltier rheometer plate (Anton Paar Physica MCR 301) and the 7-mm parallel plate tool was lowered to the measuring position (0.5 mm). A time sweep was performed within the linear viscoelastic regime (1% strain, 1 rad/sec) for 6 minutes with the Omnicure UV-365 nm light source turned on at 30 seconds and photopolymerization occurring for 5 minutes. Storage (G') and loss moduli (G") were monitored during the time sweep and the gelation point was determined at the time of crossover between the storage and loss moduli (n = 3).

To measure the mechanical properties at equilibrium swelling, BCP gels made in 6 mm syringe-tip molds were swelled in PBS (2 mL) for 2 days before performing amplitude time sweep rheology (1% strain, 1 rad/sec). Amplitude sweeps were performed for 5 minutes and storage moduli were averaged to determine the average storage modulus (n = 3).

Enzymatic Degradation of BCP Gels.

To study enzymatic degradation of hydrogels, mass loss of hydrogels incubated in collagenase solution was measured over time. Briefly, pre-swollen hydrogels were first weighed before being placed in 1.5 mL microtubes with collagenase-B solution (1 mg/mL, 1 mL). Microtubes were incubated in a 37 °C water bath to activate enzyme. Gels were removed, dried, and weighed at various time points until complete degradation was observed. Percent remaining mass was calculated at the various time points by normalizing the measured weight to the initial starting gel weight (n =3).

Cell Viability within BCP Matrices.

To evaluate cytocompatability of the block co-polymer matrices, NIH 3T3 cells were encapsulated and their viability was assessed after 1 and 5 days of culture. Briefly, 3T3 cells (4.0×10^4 cells/gel) were added to the high XL, BCP solution during photopolymerization (10 mW/cm^2, 3 min). Gels were cultured in standard DMEM media (DMEM, low glucose, 10% FBS, 1% Pen Strep) for the assigned time at 37 °C, 5% CO_2. Gels were washed with PBS and incubated for 30 min at room temperature with Live/Dead staining solution (2 µM Calcein AM and 4 µM Ethidium homodimer-1 in PBS). Gels were imaged using confocal fluorescent microscopy (Olympus FV1000) and cell viability as well as cell area were quantified using FIJI software (NIH). Fluorescent z-projections are shown for 50 slices (500 µm). For cell area, z-stack projections were manually thresholded to highlight cells and cell size was quantified using FIJI's "Analyze Particles" plugin (50 – 1000 µm^2 pixel size, 0 – 1 circularity). A lower limit of 50 µm^2 (average fibroblast cell area) was set to ensure that measurements were representative of cells fully captured within the z-stack, and an upper limit of 1000 µm^2 was set to exclude cell aggregates.

Protein Patterning on BCP Gels.

BCP precursor solution was crosslinked as previously described, but off-stoichiometry ([thiol]:[norbornene] ratio of 0.5:1) to leave residual norbornene groups for protein patterning. Subsequently, the BCP gel was immersed in a solution of L-cysteine (20 mM) and LAP (2 mM) and irradiated with UV light (10 mW/cm^2, 5 min) through a photomask in order to consume norbornene groups on one half of the gel and then rinsed in PBS. Protein conjugation to the remaining norbornene groups was then achieved using bio-orthogonal tetrazine-norbornene click chemistry. First, Texas Red ovalbumin in PBS (1.5 mg/mL) was incubated with tetrazine-N-hydroxy-succinimydl ester (Tz NHS ester, 10 equiv., synthesized as previously described[41, 42]) for 1 hr at room temperature to yield tetrazine-functionalized Texas Red ovalbumin (Tz-Tx Red Ovalbumin). Tz-Tx Red Ovalbumin (1 mg/mL) was then pipetted on top of the photopatterned BCP gel and allowed to incubate for 1 hr at room temperature to react with free norbornene groups in the unexposed (previously shielded) side of the gel. The BCP gel was then washed in PBS to remove unconjugated protein and imaged via fluorescence microscopy (Zeiss Axio Vert.A1).

Statistical Analysis.

For statistical analysis, a standard, unpaired t-test was performed for the Ellman's assay and cell studies ($p < 0.05$). A one-way ANOVA with multiple comparison using Tukey's method was performed for mechanical characterization ($p < 0.05$).

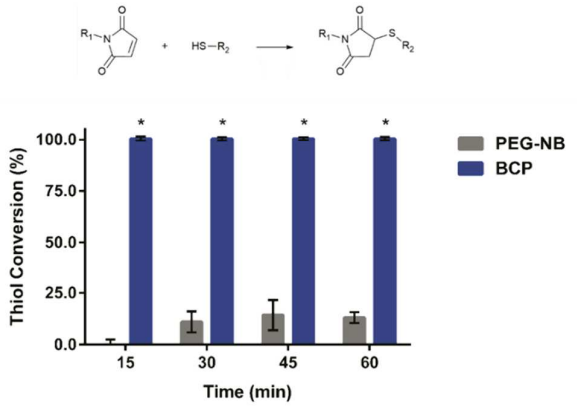

Fig. 2 Characterization of Michael Addition vs. Thiol-ene Reactions. Ellman's assay shows rapid thiol conversion for the thiol-maleimide reaction (reaction seen above) and minimal conversion for thiol-ene reaction. BCP percent thiol conversion was statistically significant compared to PEG-NB thiol conversion for all time points ($p < 0.05$, n = 3).

3. Results and Discussion

Chemical Characterization of PEG-Peptide Block Co-Polymer (BCP) Precursor and Gel. BCP precursor solution was first formed by thiol-maleimide Michael addition of PEG-di-maleimide and di-thiol peptides. Ellman's assay was used to monitor thiol conversion during Michael addition assembly of BCP chains. Absorbance results for the BCP precursor solution demonstrated complete thiol conversion after 15 minutes of reaction time. Although we did not characterize molecular weight, assuming greater than 99% conversion, we expect a degree of polymerization of 100 based on Carothers' equation for a stoichiometrically balanced step-growth polymerization.[43] Based on the relative ratios of components within the block co-polymer outlined in Table 1, the number average molecular weight would be approximately 287 kDa, and there would be an average of 35 norbornene groups per polymer chain. These estimates agree with the results of Miller *et. al.* who demonstrated high conversion of their PEG-peptide polymers via thiol-acrylate Michael addition with high molecular weight products (majority of species greater than 500 kDa).[44] Importantly, minimal thiol conversion was observed even after 60 minutes when PEG-NB was substituted for PEG-MAL (Figure 2). This result was expected since norbornene is an electron-rich alkene and should not participate in the Michael addition reaction. The partial thiol conversion in the PEG-NB solution can be attributed to di-sulfide formation of the cysteine-containing peptides.

Next, because we aimed to leverage pendant norbornenes for hydrogel crosslinking (Figure 3a), we characterized the BCP assembly by ^{1}H NMR to verify the presence of alkene related hydrogens from the norbornene groups. The results showed the characteristic norbornene peaks (5.9 – 6.3 ppm) were still present after the thiol-maleimide Michael addition but disappeared after adding a thiol source (L-cysteine) and performing thiol-ene photopolymerization (Figure 3b). Finally, we performed thiol-ene photopolymerization with a PEG-di-thiol crosslinker and used the vial tilt method to confirm that the BCP was capable of hydrogel formation (Figure 3b).

Characterization of BCP Hydrogel Mechanical Properties, Swelling, and Degradability.
After demonstrating photopolymerization of BCP chains with PEG-di-thiol and LAP, hydrogel networks were mechanically characterized via time sweep rheology to understand BCP hydrogel properties. First, *in situ* photopolymerization rheology demonstrated rapid gelation with all gel formulations exhibiting similar gel points occurring 10 seconds after photoinitiation (Supporting Information, Figure S3) and reaching a stable peak modulus after 3 - 4 min of UV-light exposure (Figure 4a). Storage modulus of pre-equilibrated BCP hydrogels decreased with increasing dilutions of BCP pre-polymer solution. Hydrogels made with the high XL formulation exhibited a storage modulus of 1036 Pa ± 43 Pa, while medium and low XL gels exhibited a storage modulus of 284 Pa ± 9 Pa and 75 Pa ± 4 Pa, respectively (Figure 4b). Additionally, swelling ratios inversely correlated with storage moduli as expected. High XL gels had a swelling ratio of 21.99 ± 0.92 while medium and low XL gels had swelling ratios of 33.49 ± 1.21 and 42.45 ± 1.58, respectively (Figure 4c). Peptide-containing hydrogels were also degraded via enzymatic degradation by collagenase-B. High XL BCP gels required 4.5

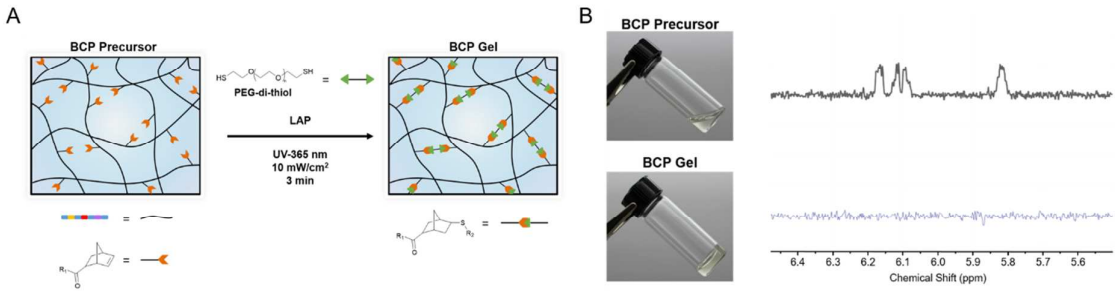

Fig. 3 BCP Gelation via Thiol-Ene Photopolymerization. (A) Schematic showing crosslinking of BCP chains through thiol-ene photopolymerization with poly(ethylene glycol)-di-thiol (PEG-di-thiol) . BCP precursor network on the left shows BCP chains that are overlapping but not crosslinked. (B) Tilt test images and corresponding ^{1}H NMR spectra show the uncrosslinked BCP precursor solution still containing the pendant norbornene groups after the thiol-maleimide reaction, while the BCP gel is crosslinked and does not contain norbornene groups after thiol-ene photopolymerization.

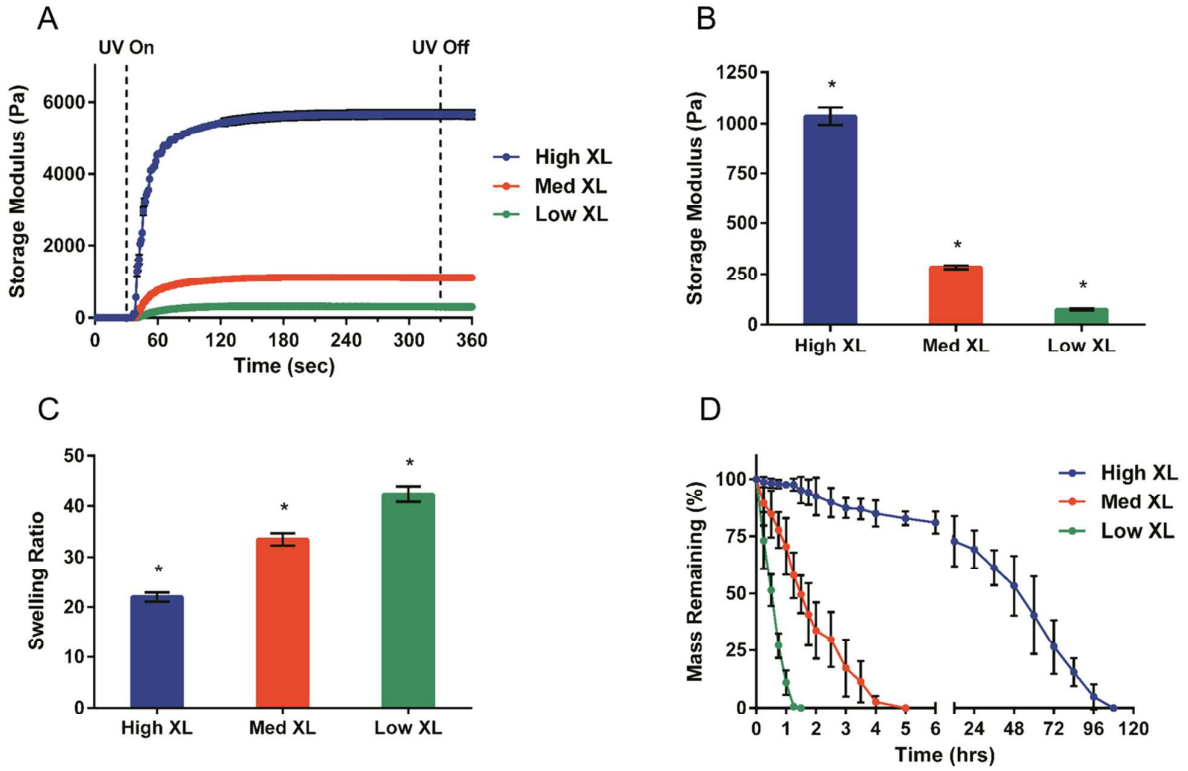

Fig. 4 Mechanical Characterization of BCP Gels. (A) *In situ* rheology showing gelation kinetics of BCP gelation at low, medium, and high crosslinking formulations. Results are averaged values over multiple runs (n = 3). (B) Storage modulus of pre-equilibrated hydrogels show a trend of decreasing modulus with lower crosslinking density, as expected. Averaged modulus values are all statistically significant with respect to each other ($p < 0.05$, n = 3). (C) Swelling ratios of hydrogels show the expected inverse correlation to the storage modulus data, with swelling ratios increasing with lower crosslinking density. Averaged swelling ratios are statistically significant with respect to each other ($p < 0.05$, n = 3). (D) Degradation of hydrogels in collagenase-B shows increased degradation time with higher crosslinking density.

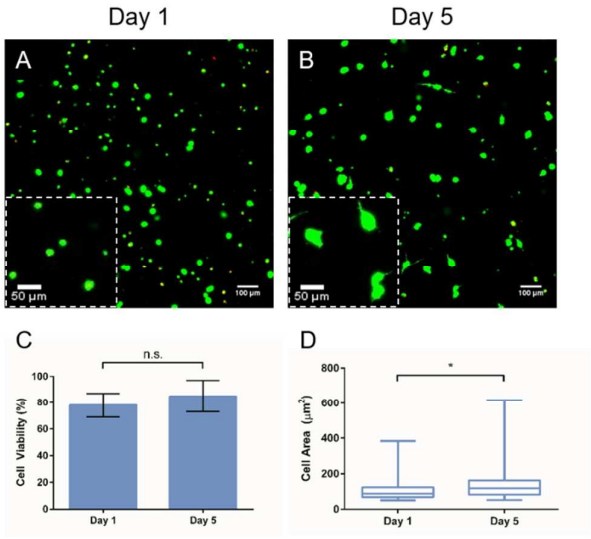

Fig. 5 Cell Encapsulation within BCP Gels. (A) Z-projection of confocal images of live/dead stained, encapsulated 3T3 fibroblasts at 1 day and (B) 5 days. The inset image shows a magnified area to better visualize cell area and spreading. (C) Analysis of live-dead images (n = 3) shows good cell viability with no difference between days 1 and 5. (D) Box and whisker plot of cell areas calculated from live-dead images (n = 3) shows a greater median and interquartile range at day 5 compared to day 1. Additionally, the average cell area is statistically different between days 1 and 5 ($p < 0.05$).

days to degrade completely, whereas medium and low XL gels degraded by 5 and 1.5 hours, respectively (Figure 4d). Taken together, these results demonstrate that BCP gels can be rapidly fabricated via photopolymerization, tuned over a range of tissue-like stiffness, and are susceptible to enzymatic degradation.

Cell Viability within BCP Hydrogels.

To demonstrate the ability of BCP gels to be cytocompatible and a platform for *in vitro* 3-D cell encapsulation, NIH 3T3 fibroblasts were encapsulated within the gels during photopolymerization. Cell viability was then assessed by Live/Dead staining with calcein AM and ethidium homodimer. Analysis of confocal fluorescent images showed 78% ± 9% cell viability after 24 hours and 85% ± 12% at 5 days, possibly due to cell proliferation (Figure 5). These results were expected given the well-established cytocompatibility of the thiol-norbornene photopolymerization reaction.[5, 6] Cell area was also quantified from confocal images and showed that average cell area statistically increased from 103 to 135 µm^2 from day 1 to day 5, respectively ($p < 0.05$). Additionally, the median and interquartile range for day 5 was larger than day 1 (119 vs. 89, and 80 vs. 55, respectively), indicating that in general the measured cell areas were overall larger on day 5 than day 1. These results were also expected given previous observations of larger cell size and spreading in enzymatically degradable

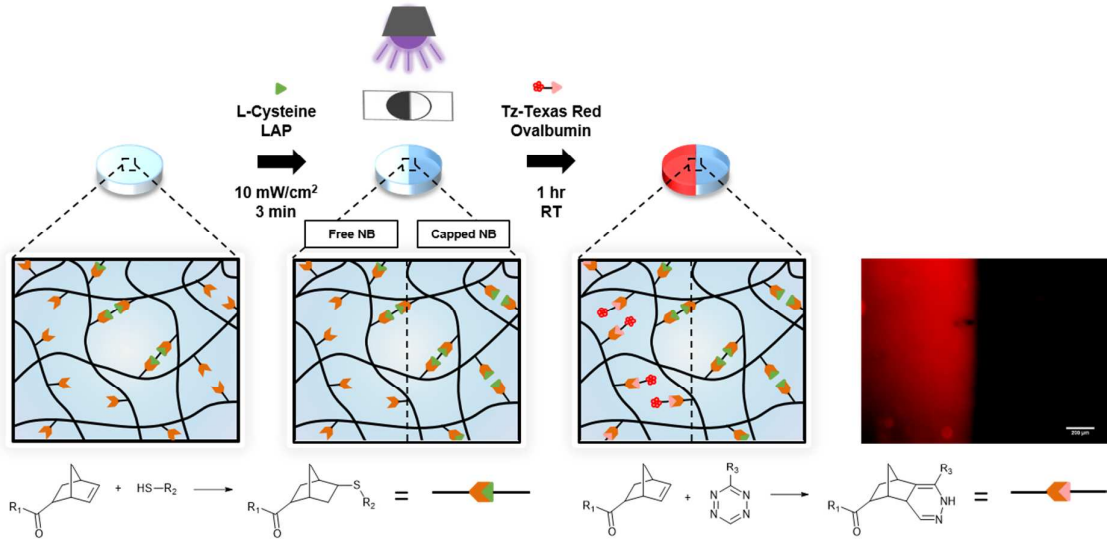

Fig. 6 Protein Photopatterning on BCP Gels. Schematic showing the step-by-step process for protein patterning. BCP gels are formed off stoichiometry, followed by thiol-ene photopolymerization with L-cysteine through a photomask, and finally protein patterning by tetrazine-norbornene click chemistry with tetrazine-functionalized protein. The fluorescent image on the right shows the resulting protein patterning with Tz-Texas Red ovalbumin on the BCP hydrogel.

PEG matrices over time.[21, 24] Also, while cell density appears to decrease between 1 day and 5 days, it was noted that BCP gels swelled considerably during culture. This could be a result of cells actively degrading the enzymatically-degradable peptide within the BCP backbone, which would cause the gels to swell in media. Despite this, BCP gels showed good cytocompatability, cell viability, and an increase in cell area throughout the bulk of the matrix.

Protein Patterning on BCP Hydrogels.

Spatial arrangement of proteins whether discretely or in gradients is of high interest for directing cellular behaviors including attachment, proliferation and differentiation.[45-49] Photolithographic techniques coupled with single or multi-photon light sources offer the ability to easily achieve spatial control in 3-D with a great degree of precision, making them widely useful for patterning of bulk hydrogels. Typically, peptide and protein-based patterning is performed by phototethering[31, 32, 50-53] or photouncaging[54-56] reactions in order to attach or uncover biological molecules, respectively. While this allows for a high degree of spatial control, exposing biologics to UV light and radical species can compromise their bioactivity, which provides an impetus for developing alternative strategies. Previous work from our lab has demonstrated the ability to sequentially perform click reactions, specifically the thiol-ene and tetrazine-norbornene click reactions, by controlling stoichiometry of reactants.[57] Advantageously, gels can initially be rapidly fabricated using radical photochemistry, while bioconjugation can be performed subsequently, without the use of an initiator, to ensure the bioactivity of sensitive proteins or growth factors. Here, we wanted to demonstrate that this approach can be extended to our BCP gels in order to spatially pattern proteins. After crosslinking BCP chains off-stoichiometry, a photomask was used to selectively cap norbornene groups in one half of the hydrogel with L-cysteine, followed by tetrazine conjugation of ovalbumin to the unexposed half. Fluorescent images showed selective fluorescent ovalbumin conjugation to only half of the BCP gel (Figure 6). Here, we still leverage the control of photopatterning by creating a "negative imprint" and then conjugate protein subsequently with a complimentary and bioorthogonal chemistry.[45] In the future, this approach could be useful for patterning bioactive growth factors for tissue engineering.

4. Conclusions

In summary, our work demonstrates that orthogonal click reactions can be leveraged to synthesize multifunctional and modular PEG-peptide hydrogels can be synthesized from simple linear precursors. The ability to tune mechanical properties within tissue-like ranges, the cytocompatability of the material platform, and the ease of protein attachment make this hydrogel platform broadly useful for tissue engineering applications. While only one BCP precursor composition was used here, the BCP gels can potentially be tailored for a desired application by manipulating the composition of the BCP components, their molecular weights, or respective working concentrations. Additionally, the ability to mix-and-match BCP precursors of various compositions adds to the versatility of these building blocks and complexity that can be obtained in the resulting BCP gels. In future studies, we will expand this platform to other synthetic precursors and peptide sequences and explore patterning bioactive proteins.

Conflicts of interest

There are no conflicts to declare.

Acknowledgements

This research was supported by the National Science Foundation (REU supplement for 1634858), the National Institute of Arthritis and Musculoskeletal and Skin Diseases of the National Institutes of Health (R21 AR071625), and start- up funds from Texas A&M Engineering Experiment Station.

References

1. A. S. Hoffman, *Adv. Drug Delivery Reviews*, 2012, **64**, 18-23.
2. K. Y. Lee and D. J. Mooney, *Chem. Rev.*, 2001, **101**, 1869-1880.
3. J. L. Drury and D. J. Mooney, *Biomaterials*, 2003, **24**, 4337-4351.
4. J. D. McCall and K. S. Anseth, *Biomacromolecules*, 2012, **13**, 2410-2417.
5. C.-C. Lin, A. Raza and H. Shih, *Biomaterials*, 2011, **32**, 9685-9695.
6. A. D. Shubin, T. J. Felong, D. Graunke, C. E. Ovitt and D. S. W. Benoit, *Tissue Eng., Part A*, 2015, **21**, 1733-1751.
7. M. Malkoch, R. Vestberg, N. Gupta, L. Mespouille, P. Dubois, A. F. Mason, J. L. Hedrick, Q. Liao, C. W. Frank, K. Kingsbury and C. J. Hawker, *Chem. Commun.*, 2006, 2774-2776.
8. S. Lee, X. Tong and F. Yang, *Biomater. Sci.*, 2016, **4**, 405-411.
9. H. C. Kolb, M. G. Finn and K. B. Sharpless, *Angew. Chem.*, 2001, **40**, 2004-2021.
10. W. H. Binder and R. Sachsenhofer, *Macromol. Rapid Commun.*, 2007, **28**, 15-54.
11. D. P. Nair, M. Podgorski, S. Chatani, T. Gong, W. X. Xi, C. R. Fenoli and C. N. Bowman, *Chem. Mater.*, 2014, **26**, 724-744.
12. C. M. Nimmo and M. S. Shoichet, *Bioconjugate Chem.*, 2011, **22**, 2199-2209.
13. S. C. Owen, S. A. Fisher, R. Y. Tam, C. M. Nimmo and M. S. Shoichet, *Langmuir*, 2013, **29**, 7393-7400.
14. C. M. Nimmo, S. C. Owen and M. S. Shoichet, *Biomacromolecules*, 2011, **12**, 824-830.
15. V. X. Truong, K. M. Tsang, G. P. Simon, R. L. Boyd, R. A. Evans, H. Thissen and J. S. Forsythe, *Biomacromolecules*, 2015, **16**, 2246-2253.
16. S. T. Koshy, R. M. Desai, P. Joly, J. Li, R. K. Bagrodia, S. A. Lewin, N. S. Joshi and D. J. Mooney, *Adv. Healthcare Mater.*, 2016, **5**, 541-547.
17. Z. Munoz, H. Shih and C. C. Lin, *Biomater. Sci.*, 2014, **2**, 1063-1072.
18. W. M. Gramlich, I. L. Kim and J. A. Burdick, *Biomaterials*, 2013, **34**, 9803-9811.
19. C. M. Magin, D. L. Alge and K. S. Anseth, *Biomed. Mater.*, 2016, **11**, 022001.
20. A. A. Aimetti, A. J. Machen and K. S. Anseth, *Biomaterials*, 2009, **30**, 6048-6054.
21. B. D. Fairbanks, M. P. Schwartz, A. E. Halevi, C. R. Nuttelman, C. N. Bowman and K. S. Anseth, *Adv. Mater.*, 2009, **21**, 5005-5010.
22. M. Lutolf and J. Hubbell, *Biomacromolecules*, 2003, **4**, 713-722.
23. M. Lutolf, J. Lauer-Fields, H. Schmoekel, A. T. Metters, F. Weber, G. Fields and J. A. Hubbell, *Proc. Natl. Acad. Sci. U.S.A.*, 2003, **100**, 5413-5418.
24. E. A. Phelps, N. O. Enemchukwu, V. F. Fiore, J. C. Sy, N. Murthy, T. A. Sulchek, T. H. Barker and A. J. Garcia, *Adv. Mater.*, 2012, **24**, 64-70, 62.
25. P. M. Kharkar, K. L. Kiick and A. M. Kloxin, *Polym. Chem.*, 2015, **6**, 5565-5574.
26. Z. Liu, Q. Lin, Y. Sun, T. Liu, C. Bao, F. Li and L. Zhu, *Adv. Mater.*, 2014, **26**, 3912-3917.
27. Y. Fu and W. J. Kao, *J. Biomed. Mater. Res., Part A*, 2011, **98**, 201-211.
28. G. N. Grover, J. Lam, T. H. Nguyen, T. Segura and H. D. Maynard, *Biomacromolecules*, 2012, **13**, 3013-3017.
29. F. Lin, J. Y. Yu, W. Tang, J. K. Zheng, A. Defante, K. Guo, C. Wesdemiotis and M. L. Becker, *Biomacromolecules*, 2013, **14**, 3749-3758.
30. J. K. Zheng, L. A. S. Callahan, J. K. Hao, K. Guo, C. Wesdemiotis, R. A. Weiss and M. L. Becker, *ACS Macro Lett.*, 2012, **1**, 1071-1073.
31. C. A. DeForest, B. D. Polizzotti and K. S. Anseth, *Nat. Mater.*, 2009, **8**, 659-664.
32. D. L. Alge, M. A. Azagarsamy, D. F. Donohue and K. S. Anseth, *Biomacromolecules*, 2013, **14**, 949-953.
33. J. Carthew, J. E. Frith, J. S. Forsythe and V. X. Truong, *J. Mater. Chem. B*, 2018, **6**, 1394-1401.
34. G. Lapienis, *Prog. Polym. Sci.*, 2009, **34**, 852-892.
35. B. K. Myers, B. Zhang, J. E. Lapucha and S. M. Grayson, *Anal. Chim. Acta*, 2014, **808**, 175-189.
36. H. Zhou, J. Woo, A. M. Cok, M. Wang, B. D. Olsen and J. A. Johnson, *Proc. Natl. Acad. Sci. U.S.A.*, 2012, **109**, 19119-19124.
37. K. Kawamoto, M. Zhong, R. Wang, B. D. Olsen and J. A. Johnson, *Macromolecules*, 2015, **48**, 8980-8988.
38. W. C. Chan and P. D. White, *Fmoc solid phase peptide synthesis : a practical approach*. Oxford University Press, 2000.
39. N. J. Anthis and G. M. Clore, *Protein Sci.*, 2013, **22**, 851-858.
40. B. D. Fairbanks, M. P. Schwartz, C. N. Bowman and K. S. Anseth, *Biomaterials*, 2009, **30**, 6702-6707.
41. N. K. Devaraj, R. Weissleder and S. A. Hilderbrand, *Bioconjug Chem.*, 2008, **19**, 2297-2299.
42. H. S. Han, N. K. Devaraj, J. Lee, S. A. Hilderbrand, R. Weissleder and M. G. Bawendi, *J. Am. Chem. Soc.*, 2010, **132**, 7838-7839.
43. W. H. Carothers, *Trans. Faraday Soc.*, 1936, **32**, 39-49.
44. J. S. Miller, C. J. Shen, W. R. Legant, J. D. Baranski, B. L. Blakely and C. S. Chen, *Biomaterials*, 2010, **31**, 3736-3743.
45. Y. Luo and M. S. Shoichet, *Nat. Mater.*, 2004, **3**, 249.
46. Y. Luo and M. S. Shoichet, *Biomacromolecules*, 2004, **5**, 2315-2323.
47. S.-H. Lee, J. J. Moon and J. L. West, *Biomaterials*, 2008, **29**, 2962-2968.
48. C. Steffen, K. S. A. and L. M. P., *Adv. Funct. Mater.*, 2009, **19**, 3411-3419.
49. D. S. Hernandez, E. T. Ritschdorff, S. K. Seidlits, C. E. Schmidt and J. B. Shear, *J. Mater. Chem. B*, 2016, **4**, 1818-1826.
50. R. G. Wylie, S. Ahsan, Y. Aizawa, K. L. Maxwell, C. M. Morshead and M. S. Shoichet, *Nat. Mater.*, 2011, **10**, 799.
51. R. G. Wylie and M. S. Shoichet, *Biomacromolecules*, 2011, **12**, 3789-3796.
52. P. E. Farahani, S. M. Adelmund, J. A. Shadish and C. A. DeForest, *J. Mater. Chem. B*, 2017, **5**, 4435-4442.

53. C. A. DeForest and D. A. Tirrell, *Nat. Mater.*, 2015, **14**, 523-531.
54. B. D. Polizzotti, B. D. Fairbanks and K. S. Anseth, *Biomacromolecules*, 2008, **9**, 1084-1087.
55. C. A. DeForest and K. S. Anseth, *Angew. Chem., Int. Ed.*, 2012, **51**, 1816-1819.
56. C. A. DeForest and K. S. Anseth, *Nat. Chem.*, 2011, **3**, 925-931.
57. F. Jivan, R. Yegappan, H. Pearce, J. K. Carrow, M. McShane, A. K. Gaharwar and D. L. Alge, *Biomacromolecules*, 2016, **17**, 3516-3523.

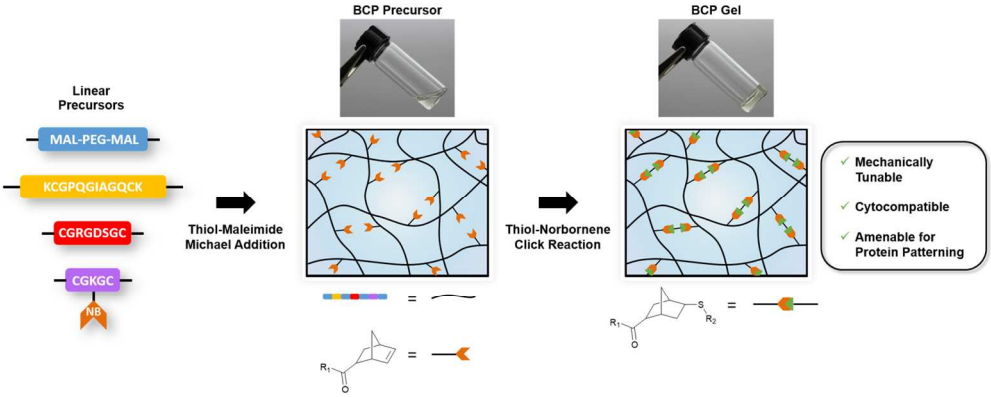

279x111mm (150 x 150 DPI)